microbiology research

MDPI

Article

Response of *Castanopsis hystrix* to the Environment, the Top Community-Building Species in Subtropical Forests: Interactions Between Rhizosphere Microbiome and Soil Metabolites

Zhuliang Jiang, Yukai Zeng, Dingping Liu and Yuanjing Li *

School of Materials and New Energy, South China Normal University, Shanwei 516600, China; 20238021007@m.scnu.edu.cn (Z.J.); 20238032034@m.scnu.edu.cn (Y.Z.); 20238021040@m.scnu.edu.cn (D.L.)
* Correspondence: liyuanjing@m.scnu.edu.cn

Abstract

Castanopsis hystrix (*C. hystrix*) is one of the most dominant and ecologically important species in subtropical evergreen broad-leaved forests of China. Interactions between its root and rhizosphere microorganisms play a pivotal role in nutrient acquisition and in mediating plant response s to environmental stresses. In this study, high-throughput 16S ribosomal RNA (16S rRNA) sequencing combined with untargeted metabolomics was employed to systematically characterize the rhizosphere microbial community and root exudates in *C. hystrix*. The results showed that, compared with non-rhizosphere soil, bacterial diversity in the rhizosphere of *C. hystrix* was significantly reduced, while several specialized and potentially efficient taxa were selectively enriched, particularly *Candidatus_Solibacter*, *Candidatus_Xiphinematobacter*, and *Candidatus_Koribacter*, thereby reshaping a distinct rhizosphere-specific community structure. Metabolomic analyses further revealed that 129 metabolites were significantly enriched in the rhizosphere, including four major classes of compounds associated with plant stress resistance: lipids and lipid-like molecules, organoheterocyclic compounds, organic acids and derivatives, and phenylpropanoids and polyketides. The enrichment of these metabolites likely contributes substantially to stress tolerance in *C. hystrix*. Kyoto Encyclopedia of Genes and Genomes (KEGG) pathway enrichment analysis identified six defense-related metabolic pathways, including pyrimidine metabolism, steroid biosynthesis, nucleotide metabolism, plant hormone signal transduction, ATP-binding cassette transporter (ABC transporters), and the biosynthesis of various plant secondary metabolites. Further correlation analysis and co-occurrence network analysis suggested that *C. hystrix* may potentially influence the enrichment of beneficial microorganisms through rhizosphere metabolites selectively, which could reduce the reliance on external nutrient acquisition and enhance the stress resilience of *C. hystrix*. Our study provides a comprehensive perspective for elucidating rhizosphere interaction networks and their ecological functions in *C. hystrix*, thereby enhancing our understanding of the environmental adaptability of dominant tree species in subtropical forests.

Keywords: *Castanopsis hystrix*; rhizosphere; root exudates; microbial community; plant stress tolerance; interactions

Check for updates

Academic Editor: Ruibo Sun

Received: 26 February 2026
Revised: 26 March 2026
Accepted: 1 April 2026
Published: 3 April 2026

Copyright: © 2026 by the authors. Licensee MDPI, Basel, Switzerland. This article is an open access article distributed under the terms and conditions of the Creative Commons Attribution (CC BY) license.

1. Introduction

The rhizosphere, defined as the narrow zone of soil directly influenced by plant roots, represents a critical interface for root–soil interactions [1,2] and a hotspot for microbial activity and specialized functional processes [3,4]. Its functional dynamics are closely linked

to plant secondary metabolism, immune responses, and overall ecological security [5]. This rhizosphere effect arises from plant adaptive responses to environmental conditions [6]. Consequently, root exudates and specific beneficial microorganisms accumulate and interact intensively within the rhizosphere, forming a tightly coupled and reciprocal network [7]. Root exudates selectively recruit and assemble microbial communities, whereas microbial metabolites, phytohormones, and other bioactive compounds modulate plant physiological processes, thereby shaping growth, defense, and the accumulation of specialized metabolites [7–9]. In turn, microorganisms regulate plant functional outputs by influencing immunity, stress tolerance, and the biosynthesis of specific metabolic products. Through these metabolically mediated interactions, the rhizosphere effect governs organic matter turnover and stabilization, maintaining the functional integrity of the rhizosphere ecosystem. Recent studies across diverse plant species have highlighted the ecological and agricultural significance of plant–rhizosphere–microbiome interactions. For instance, research on *Brassica napus* demonstrated that rhizosphere microorganisms recruited by root exudates can alter soil cadmium bioavailability, thereby influencing plant cadmium uptake [6]. In *Morus alba* cultivation systems, fertilization practices have been shown to regulate grafted plant growth adaptability by reshaping the rhizosphere microbiome and root metabolite composition [10]. Collectively, these findings underscore the importance of elucidating plant–rhizosphere–microbe interaction mechanisms to enhance nutrient cycling efficiency, safeguard ecological security, and expand species-specific application scenarios.

As a keystone species in subtropical evergreen broad-leaved forests, *C. hystrix* plays a vital role in carbon sequestration, water conservation, windbreak formation, and soil stabilization [4,11]. The ecological services provided by *C. hystrix* forests largely depend on rhizosphere microorganism-mediated biogeochemical cycling. However, the rhizosphere microenvironment of *C. hystrix* forests has been increasingly subjected to anthropogenic disturbances. On the one hand, industrial emissions and agricultural fertilization have intensified atmospheric nitrogen deposition, leading to soil acidification and suppression of beneficial soil bacteria, thereby causing microbial community imbalance in certain regions [9]. On the other hand, monoculture plantation systems with a single tree species exhibit limited nutrient-use strategies and heightened susceptibility to pests and diseases, resulting in forest degradation, reduced productivity, and increased ecosystem vulnerability. These processes further weaken ecological functions such as nitrogen fixation and nutrient transformation [12]. Such alterations disrupt rhizosphere stability in *C. hystrix* forests and ultimately impair tree growth and ecosystem health. Current studies on *C. hystrix* have primarily focused on soil microbial community structure and functional characterization. For example, Xue et al.'s research analyzed rhizosphere microbial variation along altitudinal gradients and demonstrated that elevation significantly influences soil physicochemical properties and microbial communities associated with *C. hystrix* [13]. Zhang et al.'s research on mixed forests of *C. hystrix* identified soil pH as a key environmental factor shaping bacterial and fungal community structures within soil aggregates of *C. hystrix*, elucidating the mechanisms by which mixed plantations affect aggregate-associated microbial assemblages [14]. Han et al.'s study on different ages of *C. hystrix* reported that microbial abundance dynamics generally paralleled soil nutrient dynamics, with microbial populations declining as stand age increased [15]. Nevertheless, most existing studies have focused on single microbial domains or have not systematically integrated microbiome structural shifts in the microbiome with plant metabolic responses, thereby overlooking the potential role of rhizosphere metabolites in mediating environmental adaptation in *C. hystrix* forests.

The Nanwan *Castanopsis hystrix* Provincial Nature Reserve in Guangdong Province, China, harbors the largest, most concentrated, well-preserved, and highly natural popu-

lations of *C. hystrix* in China, making it an ideal site for investigating species persistence, vegetation restoration, and high-yield cultivation techniques [16]. The study area features subtropical acidic red soil, characterized by high surface organic carbon and low available nitrogen and phosphorus [17], which is typical of natural *C. hystrix* forests in this region. However, how the rhizosphere environment of wild *C. hystrix* monocultures shapes soil bacterial community structure and metabolic functions remains insufficiently understood. Therefore, this study employs high-throughput sequencing of 16S rRNA combined with untargeted metabolomics to comparatively analyze differences in bacterial community composition and metabolic functions between rhizosphere and non-rhizosphere soils of *C. hystrix*. It aims to clarify how the rhizosphere effects of *C. hystrix* shape and regulate microbial communities, and reveal the responses of rhizosphere microbes and metabolites to environmental stress. Together, these findings provide a solid foundation for further investigation of rhizosphere interactions in dominant tree species of subtropical evergreen broad-leaved forests.

2. Materials and Methods

2.1. Study Site and Sample Collection

The Nanwan *Castanopsis hystrix* Provincial Nature Reserve in Luhu County, Guangdong Province (23°20′35″~23°21′39″ N, 115°29′52″~115°35′10″ E) covers a total area of 2890.1 hectares, with 70% of it being the most concentrated and largest area of original *C. hystrix* forest in Guangdong Province, holding significant conservation and research value [16]. The study area is characterized by subtropical acidic red soil, with high surface organic carbon content and low levels of available nitrogen and phosphorus [17], which is typical of soils in natural *C. hystrix* forests in this region.

Soil samples from the rhizosphere were collected in July 2025. The five-point sampling method was used to collect soil from 10 cm to 20 cm below the ground surface. The samples were passed through a 2–5 mm sterile sieve and then mixed evenly in equal amounts from the five sampling points in the same plot to form a composite sample, which minimizes the spatial heterogeneity of soil in the forest plot [13,14]. They were finally transported on ice to the laboratory of Majorbio Bio-Pharm Technology Co., Ltd. (Shanghai, China). Three composite rhizosphere soil samples were named HG1, HG2, and HG3, while three composite non-rhizosphere soil samples from the surrounding area were named FG1, FG2, and FG3, making a total of six soil samples.

2.2. Soil Microbial DNA Extraction, PCR Amplification, and Sequencing

Soil microbial genomic DNA was extracted from samples using the E.Z.N.A.® soil DNA Kit (Omega Bio-tek, Norcross, GA, USA) according to manufacturer's instructions. Following DNA extraction, PCR amplification was performed using primers targeting the bacterial 16S V3-V4 region (338F and 806R). The PCR reaction mixture included 20 μL Pro Tap buffer, 0.8 μL each primer (5 μM), 20 ng of template DNA, and ddH_2O to a final volume of 20 μL. PCR was performed using the following program: initial denaturation at 95 °C for 3 min, followed by 27 cycles of denaturing at 95 °C for 30 s, annealing at 55 °C for 30 s, and extension at 72 °C for 45 s, and a single extension at 72 °C for 10 min. The purified PCR products were subjected to library construction using the NEXTFLEX Rapid DNA-Seq Kit (Revvity, Inc., Austin, TX, USA) and sequenced on the Illumina Nextseq 2000 platform (Illumina, San Diego, CA, USA) [13,18].

2.3. Microbial Diversity Analysis

Raw FASTQ files were de-multiplexed using an in-house Perl script. Then, the optimized sequences were clustered into operational taxonomic units (OTUs) using UPARSE 11 at a 97% sequence similarity level. The most abundant sequence for each OTU was selected as a representative sequence. To minimize the effects of sequencing depth on alpha and beta diversity measures, the number of 16S rRNA gene sequences from each sample was rarefied to 20,000, which still yielded an average Good's coverage of 99.99%.

The taxonomy of each OTU representative sequence was analyzed by RDP Classifier version 11.5 against the 16S rRNA gene database (e.g., Silva v138) using a confidence threshold of 0.7. Bioinformatic analysis of the soil microbiota was carried out using the Majorbio Cloud platform (https://cloud.majorbio.com) [19]. Based on the OTUs information, rarefaction curves and alpha diversity indices, including observed OTUs, Chao1 richness, Shannon index, and Sobs, were calculated with Mothur v1.48.3. The similarity among microbial communities across samples was determined by principal coordinate analysis (PCoA) based on Bray–Curtis dissimilarity using Qiime v1.91. The linear discriminant analysis (LDA) effect size (LEfSe) [20] was performed to identify significantly abundant bacterial taxa (from phylum to genus) across the different groups (LDA score > 4, $p < 0.05$). A correlation between the microbiome and metabolites was considered statistically robust if Spearman's correlation coefficient was greater than 0.6 or less than −0.6, and the *p*-value was less than 0.05 [21].

2.4. Metabolite Determination

A total of 1000 mg of sample was accurately weighed into a 2 mL microcentrifuge tube, followed by the addition of one grinding bead (6 mm in diameter) and 1000 µL of extraction solvent, and 400 µL of methanol solution containing 20 µg mL^{-1} L-2-chlorophenylalanine. The mixture was then homogenized in a cryogenic tissue grinder for 6 min (−10 °C, 50 Hz), followed by low-temperature ultrasonication extraction for 30 min (5 °C, 40 kHz). Subsequently, it was kept stationary at −20 °C for 30 min and centrifuged at 13,000 rpm for 15 min at 4 °C. The supernatant was collected, dried under a gentle stream of nitrogen, and reconstituted in 120 µL of acetonitrile solution. After vortex-mixing for 30 s, the solution was extracted again by low-temperature ultrasonication for 5 min (5 °C, 40 kHz) and centrifuged again under the same conditions (13,000 rpm, 15 min, 4 °C). The final supernatant was taken for analysis. As part of the system conditioning and quality control process, a pooled quality control (QC) sample was prepared by mixing equal volumes of all samples. Detection was performed using an ultra-high-performance liquid chromatography system coupled with a Fourier-transform mass spectrometer (UHPLC-Exploris 240, Thermo Fisher Scientific, Waltham, MA, USA). Chromatographic separation was achieved on an ACQUITY UPLC HSS T3 column (100 mm × 2.1 mm i.d., 1.8 µm; Waters, Milford, CT, USA). The mobile phase consisted of (A) 95% water + 5% acetonitrile (containing 0.1% formic acid) and (B) 47.5% acetonitrile + 47.5% isopropanol + 5% water (containing 0.1% formic acid). The column temperature was 40 °C, and the injection volume was 3 µL. The optimised parameters are shown below (Table 1).

Table 1. Mass spectrometry parameters.

Parameter	Setting
Capillary voltage	Positive Ion Mode 3400 V; Negative Ion Mode 3000 V
Capillary temperature	320 °C
S-Lens RF Level	70
Acquisition range of the mass spectrum	70–1050 m/z
Sheath gas flow rate	60 arb
Aux gas flow rate	20 arb

arb: arbitrary unit, *m*/*z*: mass-to-charge ratio.

Pretreatment of LC/MS raw data was performed using Progenesis QI (Waters Corporation, Milford, CT, USA), and a three-dimensional data matrix in CSV format was exported. The information in this three-dimensional matrix included: sample information, metabolite name and mass spectral response intensity. Internal standard peaks, as well as any known false positive peaks (including noise, column bleed, and derivatized reagent peaks), were removed from the data matrix, deredundant, and peak-pooled. At the same time, the metabolites were identified by searching database, and the main databases were the Human Metabolome Database (HMDB), Metlin, and the self-compiled Majorbio Database (MJDB) of Majorbio Biotechnology Co., Ltd. (Shanghai, China). The data matrix obtained by searching the database was uploaded to the Majorbio cloud platform (https://cloud.majorbio.com) for data analysis. The R package "ropls" (Version 1.6.2) was used to perform principal component analysis (PCA) and orthogonal partial least squares discriminant analysis (OPLS-DA), and a 7-cycle interactive validation was used to evaluate the stability of the model. The metabolites with Variable importance in the projection (VIP) > 1, $p < 0.05$, Fold Change (FC) > 1.2 or <0.83 were determined as significantly different metabolites based on the VIP obtained by the OPLS-DA model and the *p*-value generated by Student's *t*-test.

The data were analyzed using the free online platform called majorbio cloud platform (cloud.majorbio.com). Differential metabolites between two groups were mapped into their biochemical pathways through metabolic enrichment and pathway analysis based on the KEGG database. These metabolites could be classified according to the pathways they are involved in or the functions they perform. Enrichment analysis was used to analyze a group of metabolites in a function node, whether they appear or not. The principle was that the annotation analysis of a single metabolite develops into an annotation analysis of a group of metabolites. Pathway enrichment analysis was performed using the Python package "scipy.stats" (version 1.0.0), and heatmaps were generated for clustering differential metabolites as well as for Spearman correlation analysis between microbiome data and metabolites.

3. Results

3.1. Changes in Rhizosphere Soil Microbial Community in C. hystrix

3.1.1. Bacterial Diversity

Plants have a significant impact on soil microbial diversity. Compared to non-rhizosphere soil, we found that in the rhizosphere soil of *C. hystrix*, the bacterial Shannon diversity index, species richness index (Chao1), and Pielou's index of species evenness were significantly lower, while the Good's coverage index was significantly higher ($p < 0.001$, Figure 1A). This indicates significant differences in richness, diversity, evenness, and coverage between the two groups. The rarefaction curve shows that the number of observed species (Sobs index) tends to plateau (Figure 1B), suggesting a reasonable sequencing

depth and sufficient coverage, and that the sequencing depth has essentially captured all detectable species in the samples.

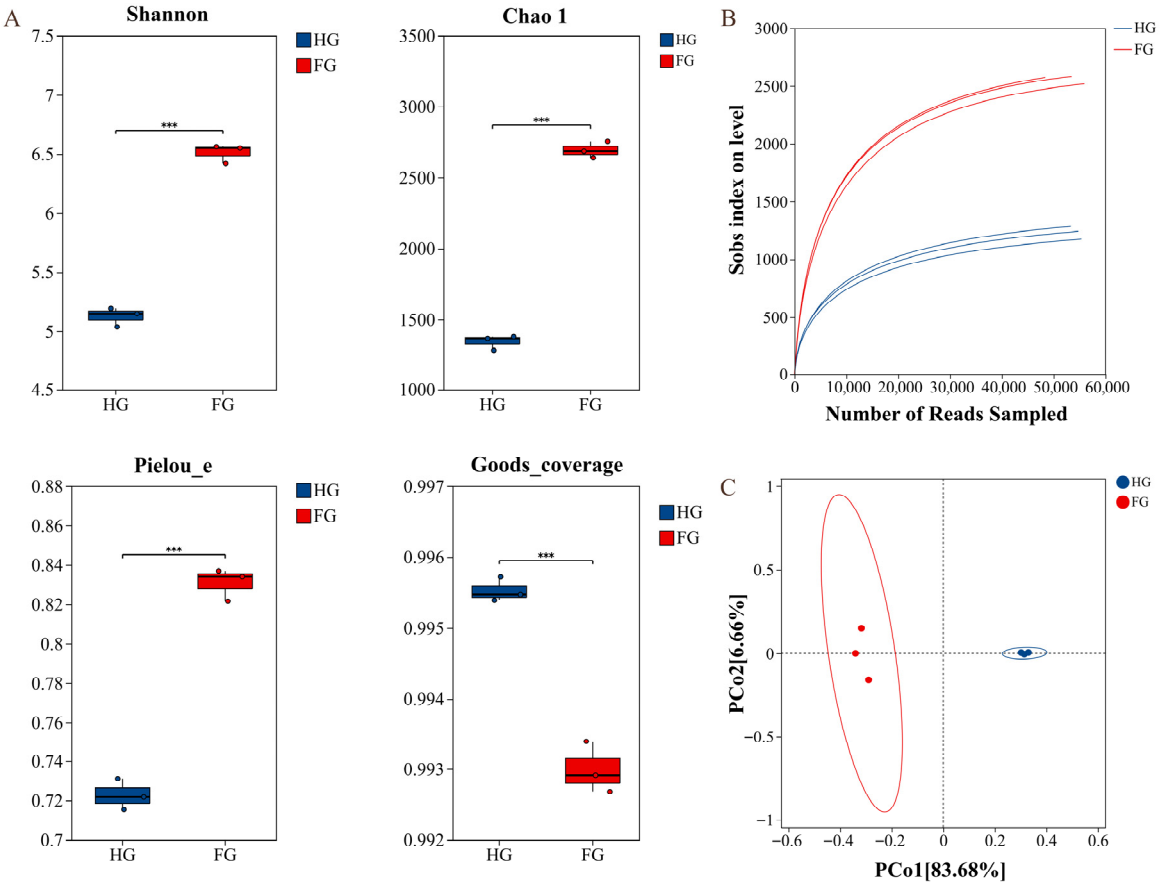


Figure 1. Alpha and beta diversity analyses of prokaryotic compositions between the two sites. (**A**) Average values of Shannon, Chao1, Goods_coverage, and Pielou_e index of OTUs. (**B**) Rarefaction curves of Sobs. (**C**) The PCoA of bacterial community composition in the rhizosphere and non-rhizosphere of *C. hystrix*. HG: rhizosphere soil of *C. hystrix*, FG: non-rhizosphere soil of *C. hystrix*. (where $p < 0.001$ is marked ***).

The PCoA results showed that the first principal coordinate (PCo1) explained 83.68% of the variation, the second principal coordinate (PCo2) explained 6.66%, and the cumulative contribution of the two principal coordinates was 90.34%, which can comprehensively reflect the sample information (Figure 1C). Rhizosphere and non-rhizosphere samples were distinctly separated, with samples within similar areas showing a clustering trend. Rhizosphere samples were more aggregated compared to non-rhizosphere samples, indicating that the unique rhizosphere environment of *C. hystrix* has a substantial influence on the structure of the soil bacterial community.

3.1.2. Bacterial Community Structure

Figure 2 shows the relative abundance of microorganisms at the phylum level (top 10) under different soil conditions. In the rhizosphere soil, the dominant phyla were *Acidobacteriota* and *Pseudomonadota*, followed by *Verrucomicrobiota*, *Actinomycetota*, and *Planctomycetota*. The dominant phyla in the non-rhizosphere soil samples were *Acidobacteriota*, *Pseudomonadota*, *Chloroflexota*, *Bacillota*, *Nitrospirota*, *Myxococcota*, and *Thermodesulfobacteriota*. Compared with the non-rhizosphere soil, the relative abundances of *Acidobacteriota*, *Pseudomonadota*, *Verrucomicrobiota*, and *Planctomycetota* in the rhizosphere were 66.2%, 23.0%, 178.4%, and 117.3% higher, respectively. In contrast, the relative abundances of *Chloroflexota*,

Bacillota, and *Actinomycetota* decreased by 55.8%, 86.7%, and 25.5%, respectively, while *Nitrospirota*, *Myxococcota*, and *Thermodesulfobacteriota* each accounted for less than 1% in the rhizosphere (Figure 2A).

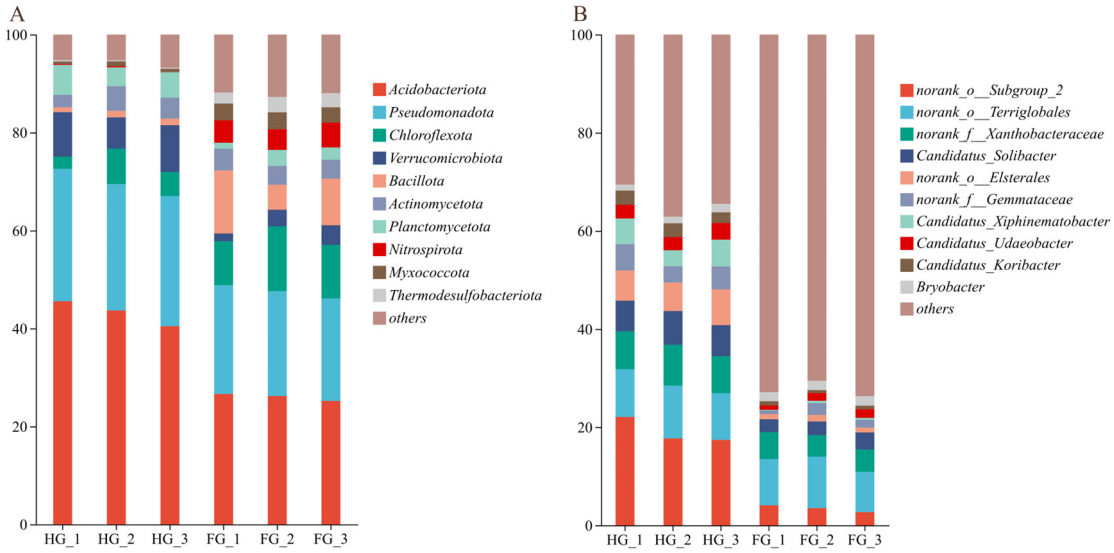


Figure 2. The relative abundance of the bacterial community at the phylum (**A**) and genus (**B**) level.

The relative abundances of the major bacterial genera in rhizosphere and non-rhizosphere soils are shown in Figure 2B. The dominant bacterial genera in the rhizosphere soil were mainly *Candidatus_Solibacter*, *Candidatus_Xiphinematobacter*. and *Candidatus_Koribacter*, each of which represented less than 1% in the non-rhizosphere soil. In addition, a considerable proportion of unclassified and non-ranked bacteria were detected in both the *C. hystrix* rhizosphere and non-rhizosphere soils. Their relative abundances were lower in the rhizosphere soil than in the surrounding non-rhizosphere soil. The "Others" category accounted for 19.43% in the rhizosphere soil, which was lower than that in the surrounding non-rhizosphere soil (48.82%). These results indicate significant differences in bacterial composition at the genus level between rhizosphere and non-rhizosphere soils and further reveal the influence of the *C. hystrix* rhizosphere environment on the structure of the soil microbial community.

3.1.3. Taxonomic Composition of Bacteria

Sequencing analysis of rhizosphere and non-rhizosphere soils from *C. hystrix* forests showed that the obtained sequence lengths ranged from 400 to 440 bp, with an average length of 414 bp. A total of 356,360 high-quality sequences were obtained, which were annotated into 3884 bacterial OTUs, belonging to 44 phyla and 633 genera. Among these, 472 OTUs were unique to the rhizosphere, while 2163 OTUs were unique to the non-rhizosphere soil (Figure 3A).

The results of LEfSe analysis for identifying differentially abundant bacterial taxa between rhizosphere and non-rhizosphere soils of *C. hystrix* are shown in Figure 3B,C. At the phylum level, the relative abundances of *Acidobacteriota*, *Planctomycetota*, *Verrucomicrobiota*, and *Pseudomonadota* were significantly higher in the rhizosphere than in the non-rhizosphere soil ($p < 0.05$, Figure 3B). In contrast, *Chloroflexota*, *Bacillota*, *Nitrospirota*, *Myxococcota*, *Bacteroidota*, and *Thermodesulfobacteriota* were more abundant in the non-rhizosphere soil ($p < 0.05$, Figure 3B). Further analysis at the genus level revealed two microbial groups whose relative abundances were significantly higher in the rhizosphere soil ($p < 0.05$, Figure 3C): *Candidatus_Solibacter* (*Acidobacteriota*) and *Candidatus_Xiphinematobacter*

(*Verrucomicrobiota*). In the non-rhizosphere soil, only *HSB OF53-F07* (*Chloroflexota*) was significantly more abundant ($p < 0.05$, Figure 3C).

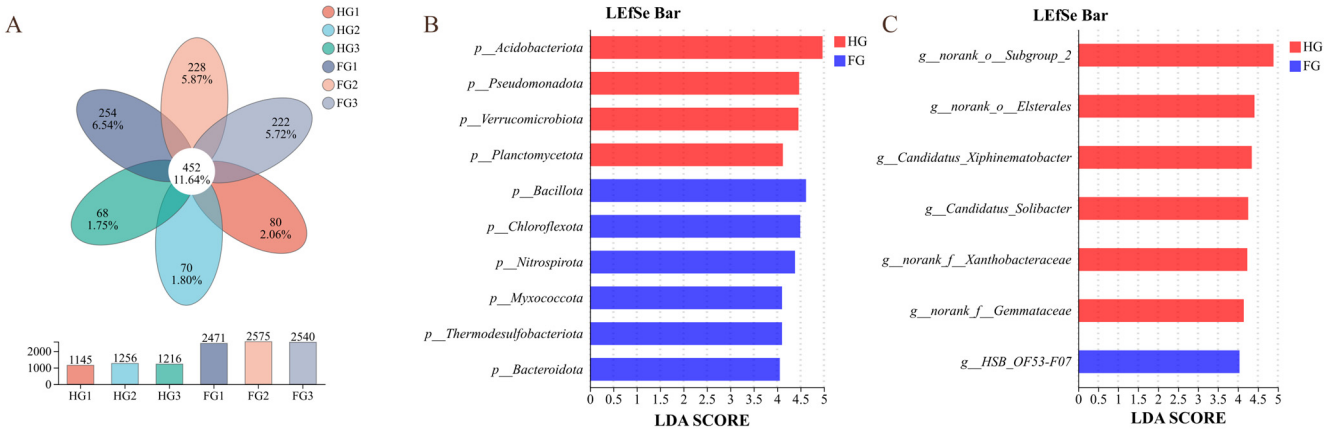


Figure 3. Classification and composition of microbial communities. (**A**) Venn diagrams illustrating the abundances of OTUs between the two sites. (**B**) Histogram of LDA value distribution of rhizosphere soil of *C. hystrix* at the phylum level; (**C**) Histogram of LDA value distribution of rhizosphere soil of *C. hystrix* at the genus level. Only taxa meeting an LDA significance threshold of 4 for bacterial communities are presented.

3.2. Differential Expression of Metabolites

3.2.1. Quality Inspection

In this experiment, 7438 positive and 5726 negative ion peaks were identified. The PCA was used to investigate the aggregation degree of the samples to prove the stability of the detection system. The QC samples in the positive and negative ion modes aggregated well, and their dispersion was significantly lower than that of the samples to be tested, indicating that the system was stable (Figure 4). The main parameters to judge the quality of the model are R^2Y (this value represents the explanation rate of the model) and Q^2 value (this value is the prediction rate of the model), which are mostly greater than 0.4 (Table 2), indicating that the OPLS-DA model is reliable. It can explain the differences between the samples of each group well.

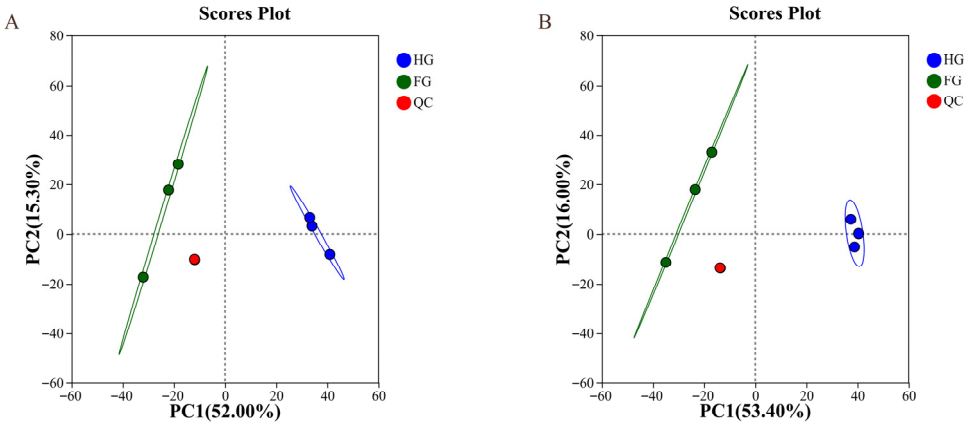


Figure 4. Principal component score map of the metabolome in different modes ((**A**) Positive and (**B**) Negative).

Table 2. OPLS-DA model parameters.

Compare	Positive Ion Mode			Negative Ion Mode		
	R^2X	R^2Y	Q^2	R^2X	R^2Y	Q^2
HG/FG	0.548	0.987	0.95	0.573	0.988	0.957

A total of 883 metabolites were detected in this study, and 378 metabolites were annotated using the database. Among them, 285 lipids and lipid-like molecules accounted for 33.06% of the total metabolites, followed by 168 organic acids and derivatives and 103 organoheterocyclic compounds, accounting for 19.49% and 11.95%, respectively (Table 3). It can be seen that lipids, organic acids, and organoheterocyclic compounds are closely related to the life activities of *C. hystrix*.

Table 3. Classification statistics of compounds in rhizosphere soil.

Superclass	Number	Percentage of Total Compound
Lipids and lipid-like molecules	285	33.06%
Organic acids and derivatives	168	19.49%
Organoheterocyclic compounds	103	11.95%
Organic oxygen compounds	99	11.48%
Phenylpropanoids and polyketides	62	7.19%
Benzenoids	58	6.73%
Nucleosides, nucleotides, and analogues	31	3.60%
Organic nitrogen compounds	20	2.32%
Not Available	17	1.97%
Lignans, neolignans and related compounds	15	1.74%
Alkaloids and derivatives	3	0.35%
Organic 1,3-dipolar compounds	1	0.12%

3.2.2. Differential Metabolites in Rhizosphere Soil Under *C. hystrix* Forest Environment

Volcano plots were used to visually compare metabolite differences between the rhizosphere and non-rhizosphere soils of *C. hystrix* (Figure 5). Metabolites with VIP > 1, $p < 0.05$ in *t*-tests, and FC > 1.2 or <0.83 were selected as differentially accumulated metabolites. In the positive ion mode, 107 metabolites showed significant differences, with 60 upregulated and 47 downregulated in the *C. hystrix* rhizosphere (Figure 5A). In the negative ion mode, 130 metabolites were significantly different, of which 69 were upregulated, and 61 were downregulated in the rhizosphere (Figure 5B). To more clearly display the relationships among rhizosphere soil samples and the expression differences in metabolites across samples, these metabolites were further subjected to cluster analysis. The heatmap results revealed that in the *C. hystrix* rhizosphere soil, 69 lipids and lipid-like molecules (45 upregulated and 24 downregulated), 15 organoheterocyclic compounds (8 upregulated and 7 downregulated), 14 organic acids and derivatives (7 upregulated and 7 downregulated), 10 phenylpropanoids and polyketides (7 upregulated and 3 downregulated), and 7 nucleosides, nucleotides, and analogues (5 upregulated and 2 downregulated) were identified (Figure 5C). The metabolites enriched in the rhizosphere are central to plant–microbe interactions. Notably, compounds such as lipids, organic acids, and phenylpropanoids have been shown to play key roles as active components of root exudates [9].

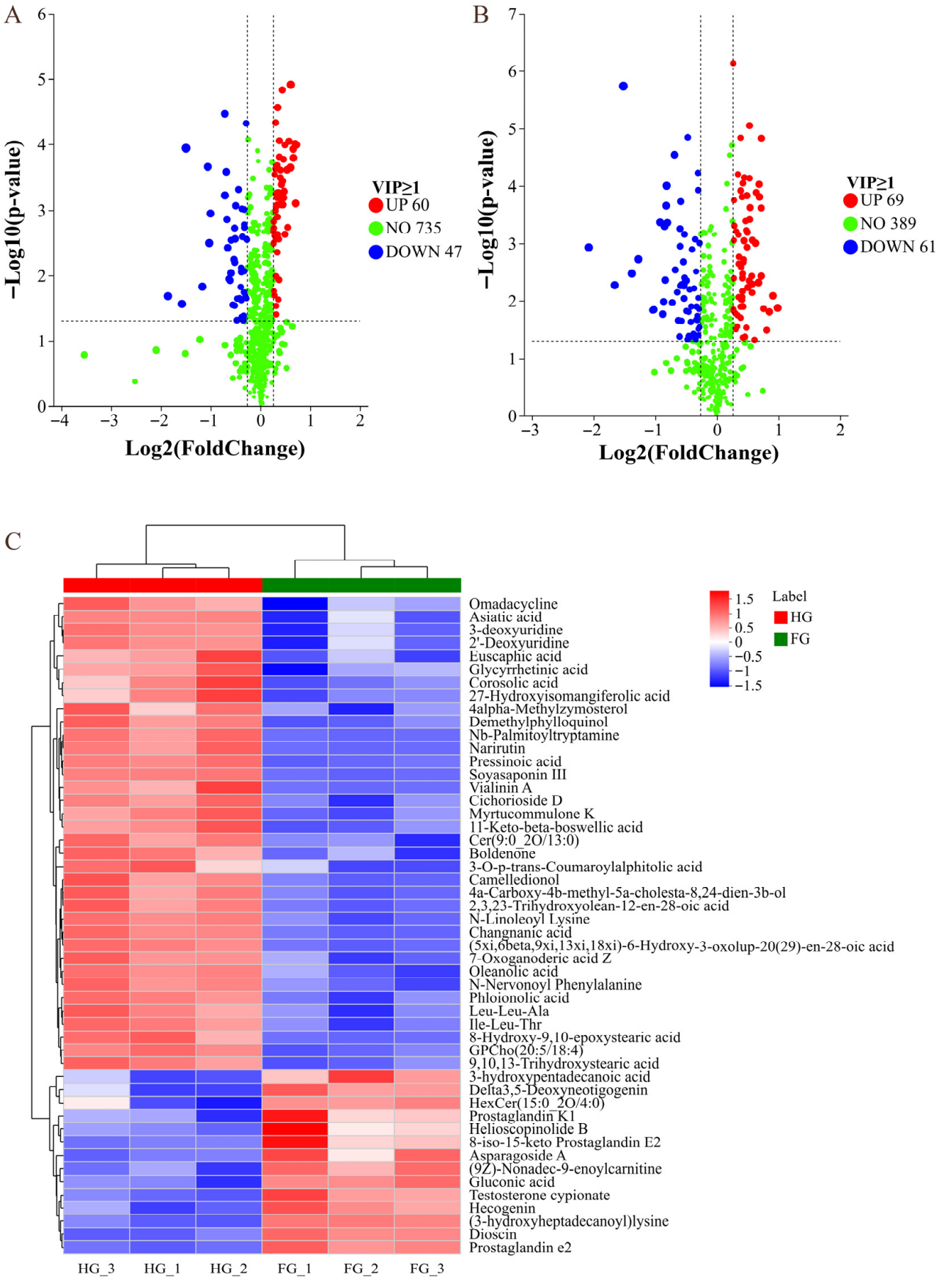


Figure 5. Screening of rhizosphere metabolites of *C. hystrix*. (**A**) Volcano plots in positive ion regulation. (**B**) Volcano plots in negative ion regulation. (**C**) Heatmap of the 50 differential metabolites that showed the most significant differences in rhizosphere of *C. hystrix*.

3.2.3. Metabolic Pathway Analysis

These differential metabolites were subjected to KEGG pathway enrichment analysis. The results (Figure 6) revealed the identification of six metabolic pathways in the *C. hystrix* rhizosphere environment: nucleotide metabolism, pyrimidine metabolism, steroid biosynthesis, ABC transporters, plant hormone signal transduction, and biosynthesis of various plant secondary metabolites. Twelve major differential metabolites were involved in the pathway enrichment. Among them, only deoxycytidine was significantly lower, while the levels of thymidine, oleanolic acid, deoxyinosine, xanthosine, 4a-carboxy-4b-methyl-5a-cholesta-8,24-dien-3b-ol, 4alpha-methylzymosterol, dihydrozeatin, protopanaxatriol, hordatine A, 2′-deoxyuridine, and brassinolide were significantly higher (Table 4).

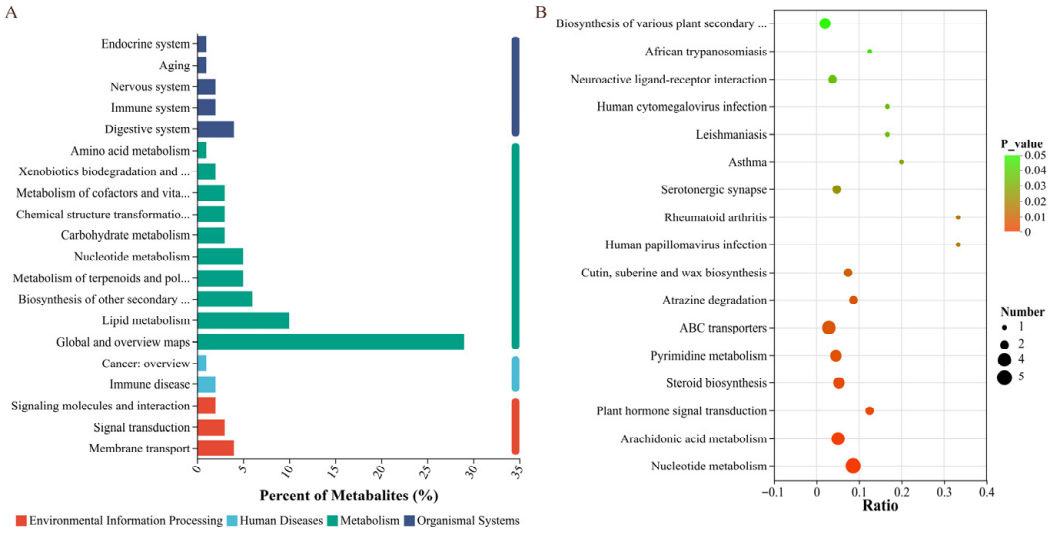


Figure 6. Functional annotation and enrichment analysis of KEGG for differential metabolites. (**A**) The bar chart displays the functional annotation of differential metabolites across various KEGG categories. (**B**) The bubble plot shows the enrichment analysis of KEGG pathways, with bubble size indicating the number of metabolites involved and color intensity representing the *p*-value for each pathway.

Table 4. Metabolic pathways of differential metabolites.

Treatment Group	Metabolic Pathways	Compounds Matching Metabolic Pathways	Significant Level of Log (p)	Impact Factor
HG/FG	Nucleotide metabolism	Thymidine Deoxycytidine Deoxyinosine Xanthosine 2′-Deoxyuridine	4.862	0.086
	Pyrimidine metabolism	Thymidine Deoxycytidine 2′-Deoxyuridine	2.263	0.045
	Steroid biosynthesis	4alpha-Methylzymosterol 4a-Carboxy-4b-methyl-5a-cholesta-8,24-dien-3b-ol	2.443	0.053
	ABC transporters	Deoxycytidine Deoxyinosine Xanthosine 2′-Deoxyuridine	2.186	0.029

Table 4. *Cont.*

Treatment Group	Metabolic Pathways	Compounds Matching Metabolic Pathways	Significant Level of Log (p)	Impact Factor
HG/FG	Plant hormone signal transduction	Brassinolide	2.477	0.125
		Dihydrozeatin		
	Biosynthesis of various plant secondary metabolites	Oleanolic acid Protopanaxatriol Hordatine A	1.325	0.020

3.3. Correlation Analysis

To evaluate the influence of root exudates on rhizosphere microorganisms, Spearman' correlation analysis was conducted between differentially abundant genera and differential metabolites in the rhizosphere and non-rhizosphere soils of *C. hystrix*. The analysis included four core microbial taxa (*Candidatus_Xiphinematobacter*, *Candidatus_Solibacter*, *Candidatus_Koribacter*, and *HSB·OF53-F07*) and 12 key functional metabolites (Table 4), aiming to clarify the association patterns between the rhizosphere metabolic environment and the microbial community. In addition, a co-occurrence network between core microbial taxa and key differential metabolites was constructed using Gephi v0.11.0 (Figure S1). The network was based on significant Spearman correlations ($|r| > 0.6$, $p < 0.05$). Nodes represent microbial genera and metabolites, and edges indicate positive (red) or negative (green) correlations. The network shows a clear modular structure. Core taxa enriched in the rhizosphere, such as *Candidatus_Xiphinematobacter* and *Candidatus_Koribacter*, cluster in a single positive module with stress-related metabolites, including dihydrozeatin, hordenine A, thymidine, and 2′-deoxyuridine. In contrast, the bulk soil-enriched group *HSB OF53-F07* forms a separate module and shows negative correlations with most rhizosphere-enriched metabolites. This modular pattern highlights specific association patterns between rhizosphere microorganisms and metabolites.

The Spearman correlation revealed significant correlations between rhizosphere-enriched taxa and specific metabolites (Figure 7). Specifically, *Candidatus_Xiphinematobacter* was strongly positively correlated with thymidine ($r = 0.99$, $p < 0.001$) and 2′-deoxyuridine ($r = 0.99$, $p < 0.001$), but negatively correlated with deoxycytidine ($r = -0.83$, $p < 0.05$). *Candidatus_Solibacter* showed significant positive correlations with brassinolide ($r = 0.94$, $p < 0.01$), dihydrozeatin ($r = 0.83$, $p < 0.05$), and hordatine A ($r = 0.83$, $p < 0.05$) while exhibiting a negative correlation with deoxycytidine ($r = -0.94$, $p < 0.01$). *Candidatus_Koribacter* was positively associated with xanthosine ($r = 0.94$, $p < 0.01$), dihydrozeatin ($r = 0.83$, $p < 0.05$), and hordatine A ($r = 0.83$, $p < 0.05$). In contrast, *HSB·OF53-F07* (Chloroflexi), which was significantly enriched in non-rhizosphere soil, was negatively correlated with xanthosine ($r = -0.82$, $p < 0.05$) and showed strong negative correlations with 4a-carboxy-4b-methyl-5a-cholesta-8,24-dien-3b-ol and 4α-methylzymosterol ($r = -0.99$, $p < 0.001$). It was also negatively correlated with brassinolide ($r = -0.89$, $p < 0.05$), dihydrozeatin ($r = -0.94$, $p < 0.01$), oleanolic acid and hordatine A ($r = -0.94$, $p < 0.01$), and protopanaxatriol ($r = -0.99$, $p < 0.001$). These significant correlations indicate statistical associations between microbial taxa and metabolites but do not demonstrate direct functional interactions or causal relationships.

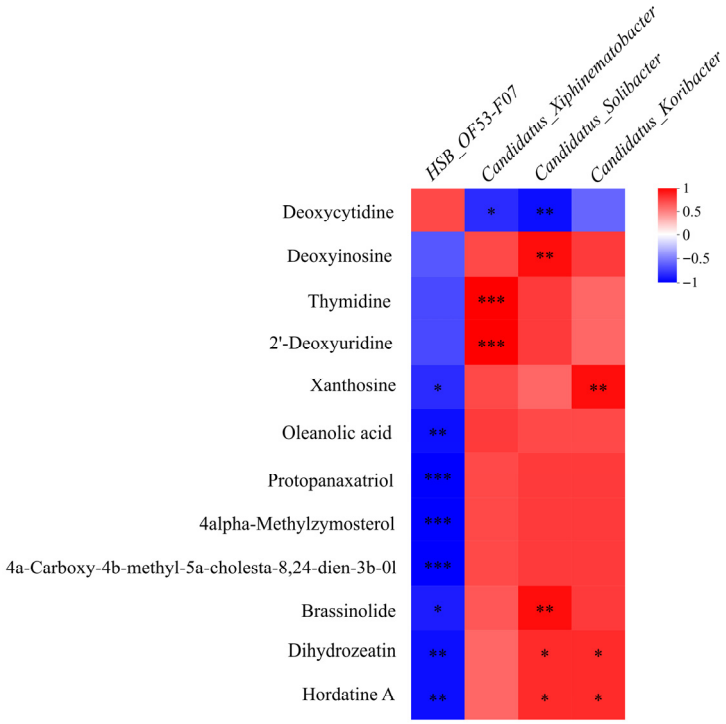


Figure 7. Correlation analysis of rhizosphere microorganisms and root metabolic products in the rhizosphere soil of *C. hystrix*. The blue color indicates a strong negative association (−1) and the red color indicates a strong positive association (+1). (where $p < 0.001$ is marked ***, $p < 0.01$ is marked **, and $p < 0.05$ is marked *).

4. Discussion

4.1. Reduced Bacterial Community Diversity Under the Influence of the C. hystrix Rhizosphere Environment

The plant rhizosphere is the site of root life activities and metabolism, and the most direct and closely interacting zone between the root and soil. Microorganisms in the plant–soil rhizosphere play a crucial role in plant growth and development [22]. As a typical forest ecosystem in the subtropics, *C. hystrix* exhibits significant differences in microbial resource distribution between its rhizosphere and non-rhizosphere zones. The results showed that the Shannon index, Chao1 index, and Pielou index of the *C. hystrix* rhizosphere soil were all lower than those of the non-rhizosphere soil (Figure 1A). This finding differs from the results reported by Li et al. [23] in their study on *C. hystrix* rhizospheres in plantations. This discrepancy likely stems from differences in soil conditions between the study areas. The soil in our study region is acidic, with a high surface organic matter content, but generally deficient in phosphorus and nitrogen [17]. A high carbon-to-nitrogen ratio can intensify microbial competition for carbon sources, allowing only a few strains adapted to low-nitrogen environments and capable of efficiently utilizing complex carbon sources to survive, thereby significantly reducing the richness and diversity of rhizosphere soil microorganisms [24]. The reduction in microbial diversity and species number in the *C. hystrix* rhizosphere soil suggests that microorganisms are gradually forming a simplified yet highly efficient strain community under the rhizosphere effect of *C. hystrix* [25]. Examples from this study include *Candidatus_Solibacter* and *Candidatus_Koribacter*, which were significantly enriched in the rhizosphere and are capable of degrading complex organic matter and promoting nitrogen and phosphorus cycling (Figure 3C). This bacterial community can enhance the rhizosphere's efficiency in acquiring specific nutrients (e.g., degradation of complex organic matter, utilization of limited nitrogen and phosphorus resources) in the short term. However, a long-term evolutionary perspective reveals that the reduction in mi-

crobial diversity in the pure *C. hystrix* forest rhizosphere may represent a trade-off strategy by the plant under specific environmental stresses (acidity, phosphorus and nitrogen deficiency). This strategy sacrifices community diversity to achieve efficient enrichment of core functional strains, thereby ensuring immediate survival needs. However, the sustainability of this strategy depends on stable environmental conditions. If soil acidification intensifies, nitrogen deposition further increases, or new environmental stressors emerge in the future, the current simplified community structure may struggle to adapt, ultimately negatively impacting the productivity and ecological service functions (e.g., carbon sequestration, soil and water conservation) of the *C. hystrix* forest.

4.2. The Rhizosphere of C. hystrix Forests Is Enriched with Highly Efficient Metabolizing Microbial Taxa

Previous studies showed that plant root exudates selectively recruited microorganisms with high carbon-use efficiency and metabolic activity, resulting in the enrichment of *Acidobacteriota* and *Pseudomonadota* in the rhizosphere [26]. *Acidobacteriota* are commonly abundant in acidic forest soils, reflecting their strong adaptation to low pH and high organic matter conditions [27]. In addition, *Verrucomicrobiota* and *Planctomycetota* play important roles in the degradation of complex carbon compounds and are often highly responsive to rhizosphere inputs [28]. Consistent with Xue's research [13], bacterial community composition in *C. hystrix* forests differs significantly between rhizosphere and non-rhizosphere soils at both the phylum and genus levels (Figure 3). At the genus level, *Candidatus_Solibacter*, *Candidatus_Xiphinematobacter*, and *Candidatus_Koribacter* are significantly enriched in the rhizosphere, likely reflecting their functional specialization in root-associated environments. *Candidatus_Solibacter* and *Candidatus_Koribacter* remain highly active in acidic forest soils characterised by low pH and limited nitrogen availability, and are capable of degrading complex organic matter, facilitating carbon transformation, and contributing to key nutrient cycles, including nitrogen and phosphorus [29]. In *C. hystrix* forests, high litter inputs combined with the continuous release of organic acids and low-molecular-weight carbon compounds from roots further promote the enrichment of these taxa, strengthening their roles in soil decomposition and nutrient cycling within the rhizosphere. Another dominant genus, *Candidatus_Xiphinematobacter*, plays a key role in nitrogen mineralization and organic matter decomposition and contributes to the stability of rhizosphere microbial communities and nitrogen utilization efficiency [30]. In contrast, the relative abundances of these functionally specialized genera were all below 1% in non-rhizosphere soils, highlighting the strong selective influence of the rhizosphere. Notably, the proportions of unclassified and non-ranked taxa are significantly lower in rhizosphere soils than in non-rhizosphere soils ($p < 0.05$, Figure 2), indicating a reduction in bacterial taxonomic richness under the influence of the *C. hystrix* rhizosphere. The reduction in diversity may limit the resilience of *C. hystrix* forests to invasion by external pathogenic microorganisms. In summary, the rhizosphere of *C. hystrix* reshapes soil microbial community structure by favoring functionally specialized taxa involved in organic matter decomposition and nutrient cycling. This selective enrichment enhances the efficiency of organic matter utilization and carbon and nitrogen uptake, thereby supporting sustained microbial activity and biogeochemical cycling under environmental stress.

4.3. Metabolic Mechanisms Underlying Rhizosphere Responses to Environmental Stress in C. hystrix Forests

In recent years, metabolomics has been widely applied in rhizosphere research and plays an important role in understanding rhizosphere processes and supporting the sustainable use and conservation of microbial resources. The rhizosphere functions as a critical interface for material exchange and energy flow between plant roots and surrounding

soil, and its physicochemical and biological properties differ markedly from those of non-rhizosphere soil [31]. Consequently, rhizosphere metabolomic analyses are essential for deep investigations of plant secondary metabolism, transcription factors, and metabolic networks. Consistent with this view, we identify a set of key metabolites that differ significantly between rhizosphere and non-rhizosphere soils of *C. hystrix* (Figure 5). Among these, 17 lipid and lipid-like molecules were significantly upregulated. These lipid and lipid-like molecules not only act as chemical signals that are exchanged for successful microbe recruitment or phytopathogen defence, but also modulate the plant's defence responses upon perception or contact with either beneficial or phytopathogenic microorganisms [32], thereby enhancing the stress tolerance of *C. hystrix*. The presence of phenylpropanoids and polyketides further suggests that *C. hystrix* may form potentially beneficial symbiotic interactions with rhizosphere microorganisms, jointly enhancing resistance to external environmental stressors [33,34]. The flavonoid compound silymonin, an organoheterocyclic metabolite, is known to enhance plant physiological performance under stress [35], and its increased production under acidic conditions suggests that the rhizosphere of *C. hystrix* may be experiencing acid stress [36]. In addition, the upregulation of the diterpene lactone andrographolide promotes reactive oxygen species scavenging, suppresses soil-borne pathogens, and supports the establishment of beneficial taxa such as *Bacillus* in the rhizosphere [37]. Similarly, the organonitrogen compound can activate plant defence mechanisms [38] and enhance plant tolerance to heavy metal contamination [39]. Finally, several small peptides detected among organic acids can selectively recruit beneficial microorganisms, further strengthening plant–microbe interactions in the rhizosphere [40].

To further clarify metabolic activity in the rhizosphere of *C. hystrix*, the identified differential metabolites are subjected to KEGG pathway analysis (Table 4; Figure 6). The results indicate that enhanced nucleotide metabolism is closely associated with the acidic conditions characteristic of the *C. hystrix* rhizosphere. This interpretation is supported by the upregulation of thymidine, xanthosine, and 2′-deoxyuridine. Thymidine supports microbial DNA repair under stress. Xanthosine contributes to energy production through oxidative phosphorylation and, through its derivatives, acts as a signaling molecule that facilitates the recruitment of beneficial microorganisms such as *Candidatus_Xiphinematobacter* [41]. In addition, 2′-deoxyuridine may expand DNA synthesis routes, allowing rhizosphere microorganisms to maintain efficient DNA production in acidic environments with limited nitrogen and phosphorus [42]. Furthermore, the upregulation of pyrimidine metabolism, a central branch of nucleotide metabolism (Table 4), provides additional biochemical support for this hypothesis: under acid stress, rhizosphere microorganisms of *C. hystrix* strengthen nucleic acid metabolism to maintain rapid growth and high metabolic activity in acidic soils. For example, the reduced abundance of deoxycytidine (Table 4) indicates substantial consumption, serving as direct evidence of intensified metabolic activity in the rhizosphere. At the same time, steroid biosynthesis was significantly enhanced in the rhizosphere of *C. hystrix* forests (Figure 6), in agreement with previous observations of microbial metabolic responses in acidic soils [43]. This enhancement was specifically reflected by the upregulation of 4alpha-methylzymosterol and 4a-carboxy-4b-methyl-5a-cholesta-8,24-dien-3b-ol (Table 4). The former serves as a key precursor of membrane sterols, accelerating cell membrane synthesis to counteract membrane damage under acidic conditions [44], whereas the latter enhances membrane stability and contributes to resistance against acid stress [45,46].

The enhancement of steroid biosynthesis highlights the importance of membrane stabilisation and stress resistance in the acidic rhizosphere environment. However, the biological functions of these lipid-derived compounds depend on their efficient intracellular trafficking and transmembrane transport. Previous studies demonstrated that ABC transporters not only facilitate the transport required for the functional activity of steroids

and lipids but also mediate the transmembrane transport of secondary metabolites and phytohormones, thereby playing important roles in plant responses to both biotic and abiotic stresses [47]. Consistent with these roles, our results demonstrate a significant activation of the ABC transporter pathway in the rhizosphere of *C. hystrix* forests (Figure 6). At the same time, the activation of plant hormone signal transduction (Table 4; Figure 6) further reflects the active regulatory response of *C. hystrix* to environmental conditions. Specifically, the upregulation of brassinolide activates the expression of stress-responsive genes [48], and regulates the expression of NHX-type $Na^+(K^+)/H^+$ antiporters, thereby alleviating ion toxicity under acidic conditions. Brassinolide also promotes the repair of damaged cell membranes and helps maintain stable membrane permeability [49]. Dihydrozeatin, a cytokinin-type phytohormone, accumulated in the rhizosphere and was associated with delayed root senescence and regulated growth and development in *C. hystrix*. In addition, dihydrozeatin promotes stomatal opening and increases leaf area, thereby enhancing photosynthetic efficiency and facilitating energy accumulation required for stress tolerance [50]. Furthermore, *C. hystrix* adapts to acidic soil conditions by enhancing the biosynthesis of diverse plant secondary metabolites, as evidenced by a significant increase in the levels of three triterpenoid compounds: oleanolic acid, hordatine A, and protopanaxatriol (Table 4). Oleanolic acid not only acts as a physical barrier against direct invasion by pathogenic microorganisms but also exhibits inhibitory effects on potentially pathogenic taxa, such as *HSB OF53-F07* (Chloroflexi) [51], which are more abundant in non-rhizosphere soils (Figure 3C). In addition, hordatine A exhibits antifungal activity [52], while protopanaxatriol serves as a key biosynthetic precursor of ginsenosides and plays an important role in plant defence mechanisms [53]. Together, these findings indicate a strong stress tolerance and potentially robust defence capacity in the rhizosphere of *C. hystrix*.

4.4. The Interaction Network Among Microorganisms, Metabolites, and Plant Stress Resistance

Correlation analysis and co-occurrence network analysis further showed that rhizosphere metabolites form selective statistical associations with functional microbial taxa. These patterns suggest potential ecological interactions between them, which may jointly contribute to the microbe-metabolite-plant interaction network in the rhizosphere of *C. hystrix*. In particular, nucleosides, nucleotides, and analogs enriched in the rhizosphere appear to be linked with specific dominant genera, suggesting that they may represent potential resources associated with these microbes. For example, *Candidatus_Xiphinematobacter* is strongly positively correlated with thymidine and 2′-deoxyuridine ($r = 0.99$, $p < 0.001$). These metabolites may meet the bacterium's needs for DNA synthesis precursors and repair compounds, particularly under acidic soil conditions [42]. Similarly, *Candidatus_Koribacter* shows a significant positive correlation with xanthosine ($r = 0.94$, $p < 0.01$), indicating a potential link to cellular energy metabolism. Its derivatives may also act as signaling molecules, potentially contributing to the co-occurrence of other beneficial microbes in the rhizosphere [41], which could be associated with the observed enrichment of *Candidatus_Koribacter*. This process may enhance the ability of *Candidatus_Koribacter* to degrade complex organic matter, thereby promoting carbon and nitrogen cycling in the rhizosphere. *Candidatus_Solibacter* is positively correlated with the plant hormones brassinolide ($r = 0.94$, $p < 0.01$) and dihydrozeatin ($r = 0.83$, $p < 0.05$), suggesting a possible association with plant hormone signal transduction. Brassinolide is known to modulate the expression of NHX-type $Na^+(K^+)/H^+$ antiporter genes, which may reduce membrane damage in *C. hystrix* under acidic stress [49]. In addition, the dihydrozeatin can delay root senescence and enhance photosynthetic efficiency. Together, these metabolites may contribute to improved physiological stress tolerance in *C. hystrix* [50]. Furthermore, *Candidatus_Solibacter* and *Candidatus_Koribacter* are significantly positively correlated with hordatine A ($p < 0.05$),

indicating that these genera may supply metabolic precursors for triterpenoid biosynthesis. The accumulation of hordatine A could be associated with the suppression of potentially pathogenic microorganisms outside the rhizosphere. In contrast, the dominant genus *HSB OF53-F07* in non-rhizosphere soil showed significant negative correlations with nucleotide-related metabolites, plant hormones, and triterpenoids ($p < 0.05$). This suggests that the bacterium may be unable to utilize the abundant nucleosides and hormones in the rhizosphere as growth substrates, and it is also highly unlikely to be able to tolerate antimicrobial substances like hordatine A, ultimately preventing its colonization of the rhizosphere. Overall, these results suggest that the rhizosphere metabolic environment of *C. hystrix* may selectively influence microbial communities, highlighting its potential role in shaping microbial community structure.

Previous studies have shown that plants, including *C. hystrix*, exhibit interactions between physiological and ecological processes in their aboveground and belowground parts. Wu et al. reported that mixing tree species affected the physiological activity of *C. hystrix* and altered the rhizosphere environment. This change allowed only certain microorganisms to persist, thereby shifting the abundance of rhizosphere microbial communities [54]. Li et al. compared phospholipid fatty acids (PLFAs) content in the rhizosphere of *C. hystrix* across different stand ages. They found a strong correlation between fine root nutrients and rhizosphere soil PLFAs, indicating a closer interaction between root exudates and microbial communities [23]. Oppenheimer-Shaanan et al. conducted experiments on *Cupressus* under drought conditions and identified that eight metabolites promoted bacterial growth and alleviated drought-induced reductions in leaf phosphorus and iron content, supporting the notion that plants can recruit beneficial microbes via metabolites under drought stress [55]. Consistent with these studies, our work also revealed strong associations between rhizosphere metabolites and microbial communities in *C. hystrix* soils, providing indirect evidence that rhizosphere metabolites may mediate the selective enrichment of beneficial microbes in *C. hystrix* forests. However, direct evidence from root exudate measurements is still lacking. Our study only represents a hypothetical functional association inferred from statistical correlations and functional potential, which requires further experimental validation for causal confirmation. Future studies using functional predictions are warranted to further explore potential interactions between microbes and metabolites and their ecological relevance.

4.5. Shortcomings and Prospects

The study investigated the interactions between the rhizosphere microbiome and metabolites of *C. hystrix* using three biological replicates, each composed of pooled samples from five collection points. This method minimized soil spatial heterogeneity and ensured that each replicate was representative. Nevertheless, the research was limited to a single representative site within the Nanwan *Castanopsis hystrix* Provincial Nature Reserve, with a limited number of independent replicates. In addition, soil physicochemical properties, such as pH, organic carbon, nitrogen, and phosphorus, are key abiotic factors influencing rhizosphere microbial and metabolic dynamics, yet these were not directly measured in our study. Finally, the analysis only revealed statistical associations between the microbiome and metabolome, without establishing direct causal relationships or functional interactions between specific microbial taxa and metabolites.

Future studies can expand sampling to multiple *C. hystrix* forest sites that differ in stand age, elevation, soil pH, and nutrient levels. This will test the consistency of rhizosphere microbiome and metabolite interaction networks and improve the generality of the results. In addition, future studies can combine soil physicochemical measurements with multi-omics analyses. This can allow quantitative evaluation of the relationships among

abiotic soil factors, microbial communities, and metabolites, providing deeper ecological insights into rhizosphere interactions. Furthermore, culture-based experiments can be used to verify causal relationships and functional interactions between core microbial taxa and key metabolites. These experiments can include isolation and purification of core microbes, in vitro metabolite assays, and pot inoculation experiments using sterile *C. hystrix* seedlings with core microbes. Metabolite manipulation can also be applied to confirm the specific roles of microbes and metabolites in mediating environmental adaptation in *C. hystrix*. Furthermore, future studies can integrate metatranscriptomics and metaproteomics with current multi-omics approaches. This can further clarify the in situ functional activity of rhizosphere microbial communities. It can also reveal how root exudates dynamically regulate the interactions between plant and microbe. Finally, long-term field monitoring and controlled pot experiments can be conducted to examine how *C. hystrix* rhizosphere systems respond and adapt to environmental disturbances such as nitrogen deposition and soil acidification. These studies can provide valuable insights for the conservation, restoration, and sustainable management of subtropical *C. hystrix* forests and associated evergreen broadleaf ecosystems.

5. Conclusions

We integrated high-throughput sequencing of 16S rRNA with untargeted metabolomics to investigate how the rhizosphere of *C. hystrix* influences soil microbial communities and associated metabolic responses. Compared with non-rhizosphere soil, the rhizosphere showed a marked reduction in microbial diversity and a shift toward a more specialized and efficient community dominated by *Candidatus_Solibacter*, *Candidatus_Xiphinematobacter*, and *Candidatus_Koribacter*, which likely enhances root-driven cycling of carbon, nitrogen, and phosphorus. Metabolomic analyses indicated that the rhizosphere was enriched in lipids, organic acids, phenylpropanoids, polyketides, and triterpenes. These changes were accompanied by the activation of six key metabolic pathways, including nucleotide and pyrimidine metabolism, steroid biosynthesis, plant hormone signaling, ABC transporters, and the biosynthesis of plant secondary metabolites. Correlation analysis and co-occurrence network analysis revealed significant statistical associations between rhizosphere-enriched microbial taxa and stress-related metabolites. These findings suggest that *C. hystrix* may selectively influence the composition of beneficial rhizosphere microbes through root-derived metabolites. In turn, these microbes may contribute to the accumulation of stress-resistant triterpenoids and other antimicrobial compounds in the rhizosphere. This reciprocal interaction appears to enhance resistance to environmental stress and points to a potential cooperative disease-resistance mechanism operating belowground. Overall, this study highlights the tight linkage between the rhizosphere microbiome and metabolome of *C. hystrix* and provides a conceptual basis for managing rhizosphere microecology in forest species growing in subtropical acidic soils.

Supplementary Materials: The following supporting information can be downloaded at: https://www.mdpi.com/article/10.3390/microbiolres17040073/s1, Figure S1: Co-occurrence network between differential metabolites and dominant microbial taxa in the rhizosphere soil of *C. hystrix*.

Author Contributions: Z.J.: Roles/Writing—original draft, Investigation, Methodology, Software, Data curation and analysis Writing—review and editing; Y.Z.: Conceptualization, Data curation, Funding acquisition, Methodology, Project administration, Writing—review and editing; D.L.: Funding acquisition, Project administration, Writing—review and editing; Y.L.: Conceptualization, Writing—review and editing. All authors have read and agreed to the published version of the manuscript.

Funding: This research was funded by the Provincial College Students' Innovative Entrepreneurial Training Plan Program (202510574105) and the Extracurricular Research Projects for Students at South China Normal University (25CLGB02).

Institutional Review Board Statement: Not applicable.

Informed Consent Statement: Not applicable.

Data Availability Statement: The 16S rRNA gene sequences presented in this study have been deposited in the National Center for Biotechnology Information (NCBI) Sequence Read Archive (SRA) public repository database under BioProject PRJNA1391889. The Metabolomics data have been deposited in MetaboLights database under accession number MTBLS13806.

Conflicts of Interest: The authors declare no conflicts of interest.

Abbreviations

The following abbreviations are used in this manuscript:

C. hystrix	*Castanopsis hystrix*
16S rRNA	16S Ribosomal RNA
OTUs	Operational Taxonomic Units
ABC transporters	ATP-Binding Cassette Transporter
PCR	Polymerase Chain Reaction
PCoA	Principal Coordinate Analysis
PCA	Principal Component Analysis
OPLS-DA	Orthogonal Partial Least Squares Discriminant Analysis
VIP	Variable Importance in Projection
FC	Fold Change
KEGG	Kyoto Encyclopedia of Genes and Genomes
LDA	Linear Discriminant Analysis
LEfSe	Linear Discriminant Analysis Effect Size
QC	Quality Control
SRA	Sequence Read Archive
NCBI	National Center for Biotechnology Information
HMDB	Human Metabolome Database
MJDB	Majorbio Database
PLFAs	Phospholipid Fatty Acids

References

1. Yang, L.; Qian, X.; Zhao, Z.; Wang, Y.; Ding, G.; Xing, X. Mechanisms of Rhizosphere Plant-Microbe Interactions: Molecular Insights into Microbial Colonization. *Front. Plant Sci.* **2024**, *15*, 1491495. [CrossRef]
2. Zhang, P.; Ding, J.; Kong, D.; Yin, H. Rhizospheric Traits and Plant Functioning Belowground. *Plant Commun.* **2026**, *7*, 101579. [CrossRef] [PubMed]
3. Xue, G.; Wu, J.; Zhou, B.; Zhu, X.; Zeng, J.; Ma, Y.; Wang, Y.; Jia, H. Effects of Shading on the Growth and Photosynthetic Fluorescence Characteristics of *Castanopsis hystrix* Seedlings of Top Community-Building Species in Southern Subtropical China. *Forests* **2023**, *14*, 1659. [CrossRef]
4. Lu, W.; Ye, J.; Li, X. Water Conservation Capacity of Litter and Soil of Pure and Mixed-Forest of *Pinus massoniana* and *Castanopsis hystrix*. *Subtrop. Agric. Res.* **2023**, *19*, 83–90.
5. Yang, Y.; Guo, L.; Li, Y.; Ji, M.; He, T.; Hou, K.; Li, J.; Zhang, H.; Shi, Z.; Zhang, H. Environmental and Rhizosphere Microbiome Drivers of Metabolic Profiles in *Gastrodia elata*: An Integrative Analysis of Soil, Metabolomics and Anti-Inflammatory Readouts. *Foods* **2025**, *14*, 4265. [CrossRef] [PubMed]
6. Wu, S.; Wu, K.; Shi, L.; Sun, X.; Tan, Q.; Hu, C. Recruitment of Specific Microbes Through Exudates Affects Cadmium Activation and Accumulation in *Brassica napus*. *J. Hazard. Mater.* **2023**, *442*, 130066. [CrossRef]

7. Shafi, Z.; Shahid, M. Root Exudates as Molecular Architects Shaping the Rhizobacterial Community: A Review. *Rhizosphere* **2025**, *36*, 101212. [CrossRef]
8. Bai, B.; Liu, W.; Qiu, X.; Zhang, J.; Zhang, J.; Bai, Y. The Root Microbiome: Community Assembly and Its Contributions to Plant Fitness. *J. Integr. Plant Biol.* **2022**, *64*, 230–243. [CrossRef]
9. Afridi, M.S.; Kumar, A.; Javed, M.A.; Dubey, A.; de Medeiros, F.H.V.; Santoyo, G. Harnessing Root Exudates for Plant Microbiome Engineering and Stress Resistance in Plants. *Microbiol. Res.* **2024**, *279*, 127564. [CrossRef]
10. Chen, X.; Fang, H.; Zhang, Y.; Liu, Z.; Qin, Y.; Cai, S.; Li, J.; Zheng, L.; Hou, Z.; Wang, X. Fertilization Alters Soil Microbiome and Root Metabolites in Grafted Mulberry (*Morus alba*) with Varied Scion-Rootstock Combinations. *Rhizosphere* **2025**, *36*, 101172. [CrossRef]
11. Li, X.; Ramos Aguila, L.C.; Luo, J.; Liu, Y.; Wu, T.; Lie, Z.; Liu, X.; Cheng, Y.; Jiang, F.; Liu, J. Carbon Storage Capacity of *Castanopsis hystrix* Plantations at Different Stand–Ages in South China. *Sci. Total Environ.* **2023**, *894*, 164974. [CrossRef]
12. Zhao, M.; Xu, L.; Wang, X.; Li, C.; Zhao, Y.; Cao, B.; Zhang, C.; Zhang, J.; Wang, J.; Chen, Y.; et al. Microplastics Promoted Cadmium Accumulation in Maize Plants by Improving Active Cadmium and Amino Acid Synthesis. *J. Hazard. Mater.* **2023**, *447*, 130788. [CrossRef]
13. Xue, G.; Xiong, J.; Tang, L.; Zhang, Q.; Zeng, J.; Zhao, C.; Wu, J.; Dong, S.; Zhu, X. Effects of Different Altitudes on *Castanopsis hystrix*, the Top Community-Building Species in Southern Subtropical China: Rhizospheric Soil Chemical Properties and Soil Microbiota. *Forests* **2024**, *15*, 187. [CrossRef]
14. Zhang, R.; Liu, Y.; Cheng, F. Impact of Tree Species Mixture on Microbial Diversity and Community Structure in Soil Aggregates of *Castanopsis hystrix* Plantations. *Microorganisms* **2025**, *13*, 578. [CrossRef] [PubMed]
15. Sheng, H.; Haider, F.U.; Aguila, L.C.R.; Khan, M.S.; Liu, J.; Li, Z.; Li, X. Structure of Microbial Communities of *Castanopsis hystrix* Plantations at Different Stand-Ages. *Pol. J. Environ. Stud.* **2025**. [CrossRef] [PubMed]
16. Liu, C.; Gong, L.; Zhang, W.; Zhong, J.; Zhang, R. Community Characteristics of *Castanopsis hystrix* Forest in Nanwan of Luhe County, Guangdong. *Chin. J. Trop. Crops* **2021**, *42*, 1499–1504. [CrossRef]
17. Zhong, J.; Huang, K.; Luo, S.; Huang, S.; Zhong, Y. Research on the Protection and Utilization of Plant Resources in Nanwan-hongzhu Forest Provincial Nature Reserve, Guangdong. *J. Green Sci. Technol.* **2023**, *25*, 44–49+93. [CrossRef]
18. Zhao, W.; Zhu, S.; Gu, B.; Yang, X.; Xia, G.; Wang, B. Effects of Cr Stress on Bacterial Community Structure and Composition in Rhizosphere Soil of *Iris tectorum* Under Different Cultivation Modes. *Microbiol. Res.* **2023**, *14*, 243–261. [CrossRef]
19. Han, C.; Shi, C.; Liu, L.; Han, J.; Yang, Q.; Wang, Y.; Li, X.; Fu, W.; Gao, H.; Huang, H.; et al. Majorbio Cloud 2024: Update Single-Cell and Multiomics Workflows. *iMeta* **2024**, *3*, e217. [CrossRef]
20. Khleborodova, A.; Gamboa-Tuz, S.D.; Ramos, M.; Segata, N.; Waldron, L.; Oh, S. *lefser*: Implementation of Metagenomic Biomarker Discovery Tool, *LEfSe*, in R. *Bioinformatics* **2024**, *40*, btae707. [CrossRef]
21. Barberán, A.; Bates, S.T.; Casamayor, E.O.; Fierer, N. Using Network Analysis to Explore Co-Occurrence Patterns in Soil Microbial Communities. *ISME J.* **2012**, *6*, 343–351, Erratum in: *ISME J.* **2014**, *8*, 952. https://doi.org/10.1038/ismej.2013.236. [CrossRef]
22. Luo, C.; He, Y.; Chen, Y. Rhizosphere Microbiome Regulation: Unlocking the Potential for Plant Growth. *Curr. Res. Microb. Sci.* **2025**, *8*, 100322. [CrossRef]
23. Li, X.; Wu, G.; Lie, Z.; Aguila, L.C.R.; Khan, M.S.; Luo, H.; Wu, T.; Liu, X.; Liu, J. Microbial Community Variation in Rhizosphere and Non-Rhizosphere Soils of *Castanopsis hystrix* Plantations Across Stand Ages. *J. For. Res.* **2025**, *36*, 82. [CrossRef]
24. Liang, Y.; Ming, A.-G.; He, Y.-J.; Luo, Y.-H.; Tan, L.; Qin, L. Structure and Function of Soil Bacterial Communities in the Monoculture and Mixed Plantation of *Pinus massoniana* and *Castanopsis hystrix* in Southern Subtropical China. *J. Appl. Ecol.* **2021**, *32*, 878–886.
25. Yin, M.Q.; Feng, J.X.; Huang, X.F.; Cai, Z.H.; Lin, G.H.; Zhou, J. Soil Microbial Community Structure in Natural and Transplanted Mangrove (*Kandelia obovata*) Forests. *Ecol. Sci.* **2016**, *6*, 35–42.
26. Ling, N.; Wang, T.; Kuzyakov, Y. Rhizosphere Bacteriome Structure and Functions. *Nat. Commun.* **2022**, *13*, 836. [CrossRef] [PubMed]
27. Jiao, F.; Qian, L.; Wu, J.; Zhang, D.; Zhang, J.; Wang, M.; Sui, X.; Zhang, X. Diversity and Composition of Soil Acidobacterial Communities in Different Temperate Forest Types of Northeast China. *Microorganisms* **2024**, *12*, 963. [CrossRef]
28. Fu, X.; Huang, Y.; Fu, Q.; Qiu, Y.; Zhao, J.; Li, J.; Wu, X.; Yang, Y.; Liu, H.; Yang, X.; et al. Critical Transition of Soil Microbial Diversity and Composition Triggered by Plant Rhizosphere Effects. *Front. Plant Sci.* **2023**, *14*, 1252821. [CrossRef]
29. Pacchioni, R.G.; Carvalho, F.M.; Thompson, C.E.; Faustino, A.L.; Nicolini, F.; Pereira, T.S.; Silva, R.C.; Cantão, M.E.; Gerber, A.; Vasconcelos, A.T.; et al. Taxonomic and Functional Profiles of Soil Samples from Atlantic Forest and Caatinga Biomes in Northeastern Brazil. *MicrobiologyOpen* **2014**, *3*, 299–315. [CrossRef]

30. Guajardo-Leiva, S.; Alarcón, J.; Gutzwiller, F.; Gallardo-Cerda, J.; Acuña-Rodríguez, I.S.; Molina-Montenegro, M.; Crandall, K.A.; Pérez-Losada, M.; Castro-Nallar, E. Source and Acquisition of Rhizosphere Microbes in Antarctic Vascular Plants. *Front. Microbiol.* **2022**, *13*, 916210. [CrossRef]
31. Sokolova, T.A. Specificity of Soil Properties in the Rhizosphere: Analysis of Literature Data. *Eurasian Soil Sci.* **2015**, *48*, 968–980. [CrossRef]
32. Macabuhay, A.; Arsova, B.; Walker, R.; Johnson, A.; Watt, M.; Roessner, U. Modulators or Facilitators? Roles of Lipids in Plant Root–Microbe Interactions. *Trends Plant Sci.* **2022**, *27*, 180–190. [CrossRef]
33. Lee, Y.J.; Rai, A.; Reuben, S.; Nesati, V.; Almeida, R.; Swarup, S. Use of Rhizosphere Metabolomics to Investigate Exudation of Phenolics by Arabidopsis Roots. In Proceedings of the EGU General Assembly Conference Abstracts, Vienna, Austria, 7–12 April 2013.
34. Kunz, C.F.; de Vries, S.; de Vries, J. Plant Terrestrialization: An Environmental Pull on the Evolution of Multi-Sourced Streptophyte Phenolics. *Philos. Trans. R. Soc. B* **2024**, *379*, 20230358. [CrossRef]
35. Rady, M.M.; Alharby, H.F.; Tarfayah, D.; Ahmed, S.M. Acidified Compost and Silymarin-Enriched Bio-Stimulators Integratively Improve Morpho-Physio-Biochemistry, Antioxidant Capacity, and Polyamine Metabolism Enzymes of *Atriplex nummularia* Lindl Seedlings Under Saline-Calcareous Conditions. *J. Soil Sci. Plant Nutr.* **2023**, *23*, 4669–4690. [CrossRef]
36. Rahimi, S.; Hasanloo, T. The Effect of Temperature and pH on Biomass and Bioactive Compound Production in Silybum Marianum Hairy Root Cultures. *Res. J. Pharmacogn.* **2016**, *3*, 53–59.
37. Kumari, P.; Shanker, K.; Singh, A. Insight into *Andrographis paniculata* Associated Bacterial Endomicrobiome and Assessment of Culturable Bacterial Endophytes for Enhancement of Industrially Important Andrographolide Content. *Ind. Crops Prod.* **2023**, *200*, 116840. [CrossRef]
38. Laurell, C.; Berglund, T.; Ohlsson, A.B. Transcriptome Analysis Shows Nicotinamide Seed Treatment Alters Expression of Genes Involved in Defense and Epigenetic Processes in Roots of Seedlings of *Picea abies*. *J. For. Res.* **2022**, *33*, 1365–1375. [CrossRef]
39. Yılmaz, H.; Çiftçi, V. Enhancing Cadmium Tolerance in Common Bean Plants by Seed Priming with Putrescine. *Black Sea J. Agric.* **2025**, *8*, 9–10. [CrossRef]
40. Tan, W.; Nian, H.; Tran, L.-S.P.; Jin, J.; Lian, T. Small Peptides: Novel Targets for Modulating Plant–Rhizosphere Microbe Interactions. *Trends Microbiol.* **2024**, *32*, 1072–1083. [CrossRef] [PubMed]
41. Liu, H.; Su, Y.; Ye, C.; Zuo, D.; Wang, L.; Mei, X.; Deng, W.; Liu, Y.; Huang, H.; Hao, J.; et al. Nucleotides Enriched Under Heat Stress Recruit Beneficial Rhizomicrobes to Protect Plants from Heat and Root-Rot Stresses. *Microbiome* **2025**, *13*, 160. [CrossRef] [PubMed]
42. Wang, P.; Wang, C.; Wang, Y. Nucleotide Salvage, Genome Instability, and Potential Therapeutic Applications. *Nucleic Acids Res.* **2026**, *54*, gkag099. [CrossRef]
43. Shu, S. Study on the Acid Tolerance Mechanism of *Klebsiella quasipneumoniae* Y41 and Its Ameliorative Effects on Acidic Purple Soils in Chongqing. Master's Thesis, The Southwest University, Chongqing, China, May 2025.
44. Elsaman, H.; Golubtsov, E.; Brazil, S.; Ng, N.; Klugherz, I.; Martin, R.; Dichtl, K.; Müller, C.; Wagener, J. Toxic Eburicol Accumulation Drives the Antifungal Activity of Azoles Against *Aspergillus fumigatus*. *Nat. Commun.* **2024**, *15*, 6312. [CrossRef]
45. Ren, L.; Zha, H.; Zhang, Q.; Xie, Y.; Li, J.; Hu, Z.; Tao, X.; Xu, D.; Li, F.; Zhang, B. Altered Sterol Composition Mediates Multiple Tolerance of *Kluyveromyces marxianus* for Xylitol Production. *Microb. Cell Factories* **2024**, *23*, 271. [CrossRef] [PubMed]
46. Ferraz, L.; Vorauer-Uhl, K.; Sauer, M.; Sousa, M.J.; Branduardi, P. Impact of Ergosterol Content on Acetic and Lactic Acids Toxicity to *Saccharomyces cerevisiae*. *Yeast* **2023**, *40*, 152–165. [CrossRef] [PubMed]
47. Devi, R.; Arora, P.; Verma, B.; Hussain, S.; Chowdhary, F.; Tabssum, R.; Gupta, S. ABCB Transporters: Functionality Extends to More than Auxin Transportation. *Planta* **2025**, *261*, 93. [CrossRef]
48. Gao, Y.; Ma, X.; Zhang, Z.; Wang, X.; Wang, Y. Brassinolides Signaling Pathway: Tandem Response to Plant Hormones and Regulation Under Various Abiotic Stresses. *Hortic. Adv.* **2024**, *2*, 27. [CrossRef]
49. Su, Q.; Zheng, X.; Tian, Y.; Wang, C. Exogenous Brassinolide Alleviates Salt Stress in *Malus hupehensis* Rehd. by Regulating the Transcription of NHX-Type $Na^+(K^+)/H^+$ Antiporters. *Front. Plant Sci.* **2020**, *11*, 38. [CrossRef]
50. Rathore, R.S.; Mishra, M.; Pareek, A.; Singla-Pareek, S.L. Concurrent Improvement of Rice Grain Yield and Abiotic Stress Tolerance by Overexpression of Cytokinin Activating Enzyme LONELY GUY (OsLOG). *Plant Physiol. Biochem.* **2024**, *211*, 108635. [CrossRef]
51. El Ghallab, Y.; Dakir, M.; Aainouss, A.; El Messaoudi, M.D.; Derfoufi, S. Oleanolic Acid: An Antimycobacterial Component of *Syzygium aromaticum* L. and Inhibitor of Efflux Mediated Drug Resistance. *Nat. Prod. Res.* **2025**, *39*, 4585–4591. [CrossRef]
52. Ube, N.; Ishihara, A.; Yabuta, Y.; Taketa, S.; Kato, Y.; Nomura, T. Molecular Identification of a Laccase That Catalyzes the Oxidative Coupling of a Hydroxycinnamic Acid Amide for Hordatine Biosynthesis in Barley. *Plant J.* **2023**, *115*, 1037–1050. [CrossRef]
53. Ma, L.-J.; Liu, X.; Guo, L.; Luo, Y.; Zhang, B.; Cui, X.; Yang, K.; Cai, J.; Liu, F.; Ma, N.; et al. Discovery of Plant Chemical Defence Mediated by a Two-Component System Involving β-Glucosidase in *Panax* Species. *Nat. Commun.* **2024**, *15*, 602. [CrossRef] [PubMed]

54. Wu, Y.; Zhang, S.; Xie, G.; Shao, Y.; Shi, S.; Lin, J.; Mao, Q.; Li, Y. Response of Leaf Functional Traits and Rhizosphere Microbial Communities of *Castanopsis hystrix* in Three Subtropical Plantations with Leguminous or Non-Leguminous Trees. *Forests* **2025**, *16*, 367. [CrossRef]
55. Oppenheimer-Shaanan, Y.; Jakoby, G.; Starr, M.L.; Karliner, R.; Eilon, G.; Itkin, M.; Malitsky, S.; Klein, T. A Dynamic Rhizosphere Interplay Between Tree Roots and Soil Bacteria Under Drought Stress. *eLife* **2022**, *11*, e79679. [CrossRef] [PubMed]

Disclaimer/Publisher's Note: The statements, opinions and data contained in all publications are solely those of the individual author(s) and contributor(s) and not of MDPI and/or the editor(s). MDPI and/or the editor(s) disclaim responsibility for any injury to people or property resulting from any ideas, methods, instructions or products referred to in the content.